Title
Budburst and leaf area expansion measured with a ground-based, mobile camera system and simple color thresholding

Journal
Center for Embedded Network Sensing, 65

Author
Graham, Eric

Publication Date
2008

DOI
10.1016/j.envexpbot.2008.09.013

Peer reviewed

Environmental and Experimental Botany 65 (2009) 238–244

Contents lists available at ScienceDirect

Environmental and Experimental Botany

journal homepage: www.elsevier.com/locate/envexpbot

Budburst and leaf area expansion measured with a novel mobile camera system and simple color thresholding

Eric A. Graham[a], Eric M. Yuen[a], Geoff F. Robertson[b], William J. Kaiser[a,c], Michael P. Hamilton[a,d], Philip W. Rundel[a,e,*]

[a] Center for Embedded Networked Sensing, University of California, Los Angeles, 3563 Boelter Hall, Los Angeles, CA 90095-1596, USA
[b] Department of Biology, University of California, Riverside, Riverside, CA 92521, USA
[c] Electrical Engineering Department, University of California, Los Angeles, CA 90095-1594, USA
[d] James San Jacinto Mountains Reserve, University of California, Post Office Box 1775, Idyllwild, CA 92549-1775, USA
[e] Department of Ecology and Evolutionary Biology, University of California, Los Angeles, CA 90095-1606, USA

ARTICLE INFO

Article history:
Received 3 September 2008
Accepted 24 September 2008

Keywords:
Digital camera
Green-up
Robotic
HSL color space

ABSTRACT

Plant phenology relates strongly to primary productivity and the energy that enters into ecological food webs, and thus is vital in understanding ecosystem function and the effects of climate and climate change. The manual collection of phenological data is labor-intensive and not easily scalable, thus the ability to quantify leaf flush and other parameters at many locations requires innovative new methodologies such as the use of visible light digital cameras. Improved imaging performance was obtained by using a cabled, mobile camera system that allowed a repeated image census of branches of *Rhododendron occidentale* in the understory along a 30 m transect during leaf flush. Automatic division of acquired images into areas of interest (leaves) and background for calculating leaf area was accomplished by thresholding images in different color spaces. Transformation of the color space into the hue, saturation, and luminance (HSL) color space before thresholding resulted in a mean RMS error of 21.2 cm^2 compared to hand-counts of leaf area. Thresholding in the native red, green, and blue (RGB) color space to isolate leaves resulted in a larger error, as did using algebraic combinations of the color components or color ratios. Relating physiological function to images, as for sap flow for branches of *R. occidentale*, indicates that the greening and calculated leaf area of a species as detected by imagers requires additional meteorological sensor data for interpretation.

1. Introduction

Plant phenology is one of the most responsive and easily observable traits in nature that are impacted by changing climate (Badeck et al., 2004). Measurements of plant phenology can provide an important means of understanding the dynamic relationships between primary productivity, competition between plant species, the interactions with other organisms, and the periodic phenomena that drive them (Wright et al., 1999). Indeed, interest in plant phenology and global climate change has increased significantly in recent years, especially with estimates of the advancing initiation of spring activity by both ground-based observations (Walther et al., 2002; Root et al., 2003) and by satellite (Slayback et al., 2003; Stöckli and Vidale, 2004). The new U.S. National Phenology Network (NPN, www.usanpn.org; Betancourt et al., 2007) is devoted to observing continental-scale trends in plant systems and growth dynamics.

The best tools to observe large-scale changes in phenological patterns with climate change are remote sensing applications that are linked to ground-based measurements. But scaling of ground-based measurements for validation of remote sensing data is difficult, not only because such measurements are labor-intensive but also because phenological events are usually unevenly distributed and the quality of ground-based data is often dependent on a qualitative observer (Menzel, 2002). Attempts are being made to add new technology to scaling up of processes (Allen et al., 2007), to standardize such ground-based measurements by using a subset of species (NPN), and by modeling local climatic conditions (Jolly et al., 2005). Methods for scaling up ground-based measurements are still lacking, however, and the use of visible light digital cameras holds promise (Richardson et al., 2007).

Obstacles in natural situations present particular problems for sensing. For imaging, a prohibitively high density of cameras would be required to guarantee sensing performance in an unknown and

* Corresponding author.
E-mail address: rundel@ucla.edu (P.W. Rundel).

0098-8472/$ – see front matter © 2008 Elsevier B.V. All rights reserved.
doi:10.1016/j.envexpbot.2008.09.013

changing environment, although use of multiple, small cameras has been explored (Rahimi et al., 2006). An alternative is to use a system to re-position a single camera in response to environmental obstacles or dynamic growth. The use of mobility to increase the range and granularity of a sensor has been investigated in a number of ecological situations (Harmon et al., 2007; Caron et al., 2008). Even a small range of mobility relative to the mean obstacle size of the environment can lead to significant improvement in coverage performance (Kansal et al., 2003). Thus, standard pan-tilt-zoom (PTZ) cameras, or those with even greater mobility, will have greater capability in tasks such as phenological monitoring than stationary imagers.

In addition to camera mobility, the automatic or semi-automatic analysis of images is of great utility in data reduction. Recently, algebraic combinations of the red, green, and blue (RGB) color components of images have been used in studies that combine imaging and plant physiology. These studies range from detecting CO_2 fluxes in a desiccation-tolerant moss (Graham et al., 2006; Hyman et al., 2007) to those in large, mixed stands of deciduous trees (Richardson et al., 2007). This method is attractive because calculating color ratios in an image is straightforward and many open-source software packages have functions that facilitate this analysis (e.g., Python, R). However, a large disadvantage to such color-based automated analysis is that a subset of the entire image, often a manually select area of interest, is often needed, and thus reduces the desired signal contained in the image or requires extensive manual processing.

Automatic division of images into areas of interest (segmentation) can be accomplished in many ways (Cheng et al., 2001; Litwin et al., 2001). A simple method is to automatically isolate areas of interest based on color thresholding, where pixel values above or below a determined value in each color component are excluded from the area of interest. Such automatically determined areas of interest can then be quantified by counting the enclosing pixels or by using only those selected areas for algebraic color analysis. Working in the RGB color space is attractive because it is the native system of many image capture systems. However, the transformation of the color space into the hue, saturation, and luminance (HSL) color space, a simple to implement function, allows for better color constancy with the changing light conditions that may have occurred during image capture (Liu and Moore, 1990; Bruce et al., 2000).

This study examines the potential for using both a mobile camera and color thresholding of the images it captured in determining the dynamics of expanding leaf area for *Rhododendron occidentale*, a deciduous understory shrub. Portions of this hardware and software system are part of several existing and proposed ecological observatory networks (Hamilton et al., 2007). It was hypothesized that the mobile camera would allow the quantification of the leaf area of multiple branches that would have been occluded from a single viewpoint and that automatic color segmentation would produce a sufficiently strong signal to accurately estimate leaf area from images.

2. Materials and methods

2.1. Field site and manual measurements

The University of California James Reserve (www.jamesreserve.edu) is located in the San Jacinto Mountains of southern California (33° 48′ 30″ N, 116° 46′ 40″ W) at 1658 m elevation in a mixed conifer and hardwood forest with a perennial mountain stream. The area receives a mean of 485 mm precipitation annually. The reserve acts as a testbed for technology developed by the Center for Embedded Networked Sensing (CENS; http://research.cens.ucla.edu), an NSF-funded Science and Technology Center located at the University of California, Los Angeles.

The stand of *Rhododendron occidental* under investigation occurred on an approximately 20° slope near a small permanent stream. Individual heights varied from about 1.5 to 2 m in height and the area dominated by this species was approximately 150 m^2. The overstory was relatively uniform and disperse and consisted of approximately 20 m tall *Pinus ponderosa* and mixed conifers.

Leaf number, lengths, and widths were hand-collected for 36 target branches in 2004 and 18 branches of *R. occidentale* in 2005. Branches were loosely tied to 2 m metal posts driven into the soil to reduce their movement and facilitate imaging. Leaves were measured with a small ruler approximately weekly from the beginning of May until about mid-July for both years. Leaf area was determined from a linear regression ($r^2 = 0.98$) of leaf width × length against leaf area measured photographically in the lab, using a freely available image-processing tool (Scion Image, Scion Corporation, Frederick, Maryland, USA) run on a personal computer. Collar-type sap flow probes (model SGA5-WS, Dynamax Inc., Houston Texas, USA) were placed on two branches in 2005 to measure hydraulic transport of the branch xylem system in relation to leaf expansion. Sap flow data were collected every 5 min from the beginning of May through the end of August by a datalogger (CR23X, Campbell Scientific, Inc., Logan, Utah, USA).

2.2. Mobile camera system

The Networked Infomechanical Systems (NIMS) family of cable-based robotic systems, developed at the Department of Electrical Engineering at the University of California, Los Angeles (UCLA), includes a system that is rapidly deployable and has been used for a variety of environmental monitoring applications (Harmon et al., 2007; Caron et al., 2008). Developed to complement fixed sensor deployments, it provides high precision and reliable mobility to locate and move a payload of sensors along a horizontal transect in pre-programmed or adaptive sampling (Zhang and Sukhatme, 2007) schedules, with vertical movement also possible (Fig. 1; Pon et al., 2005; Jordan et al., 2007).

The mobile capability is accompanied by many challenges, including optimizing the spatiotemporal components of sampling; however the ability to rapidly deploy the cabled system and auto-

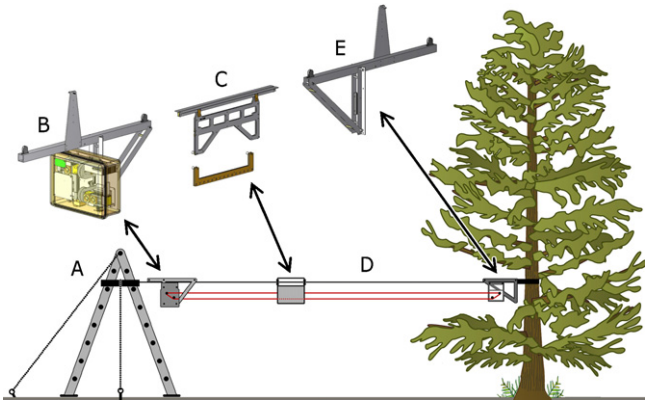

Fig. 1. The robotic system, Networked Info-Mechanical Systems (NIMS), designed to move payloads, such as sensors or cameras, along a horizontal transect. Components include: (A) a rapidly deployed support structure, (B) a motor box that controls horizontal and vertical (if equipped) movement of the shuttle, (C) a shuttle onto which sensors can be mounted and that is moved along the transect by a continuous horizontal drive cable and is supported by (D) the weight bearing cable, and (E) the end anchor and return pulley for the horizontal drive cable that hangs from the support cable.

matically and adaptively relocate sensing equipment has proved to significantly increase sensing system performance (Rahimi et al., 2005). The system in use at the James Reserve was a prototype of the systems currently in production (Fig. 1) and included an Ethernet-connected, pan-tilt-zoom (PTZ) camera (Model VB-C10R, Canon U.S.A., Inc., Irvine, California USA) that was periodically positioned along a 30 m transect to capture obstruction-free images of the target branches of *R. occidentale*.

At each location, the PTZ of the camera was also adjusted. Images were manually captured of target branches in June and July of 2004 and then again from May through July 2005. Captured images were stored on an onboard, small form-factor computer (model type PC/104, Advanced Digital Logic, San Diego, California, USA) and then were transferred wirelessly by Secure Shell (SSH) protocol to a local computer at UCLA. Subsequently, images were archived in an open source database (MySQL Inc., Cupertino, California, USA) with a custom front-end designed to facilitate the sharing of sensor data (SensorBase, www.sensorbase.org; Chang et al., 2006).

2.3. Image processing

Images captured by the NIMS camera had a resolution of 480 by 768 pixels and were stored as uncompressed bitmaps encoded using the Joint Photographic Experts Group (JPEG; ITU, 1992) algorithm. Images were either maintained in their native RGB color space or were transformed to HSL (Pratt, 2001), scaling each color component to an integer between zero and 255, prior to segmentation. The hue, saturation, and luminance (HSL) color space describes a cylinder (as opposed to the RGB cube) whose central axis corresponds to luminance, which ranges from black (value is zero) to white (value is 255), the angle around this axis corresponds to hue (value ranges from zero to 255, or sometimes to 360°), and the distance from the axis corresponds to saturation (value ranges from zero at the axis for neutral grays to 255 at the edge of the cylinder for the completely saturated colors of "red", "orange", "violet" etc.). Thus, any color can be represented using the three values of hue, saturation, and luminance, similar to representing any color as a red, green, and blue value in the RGB color space. Selected images in both color spaces were segmented into regions of interest (leaves) and non-interest (background) using a custom-built, web-based tool that allowed the visual and interactive selection of areas of interest based on thresholds of the color components (e.g., areas of interest could be defined as those with red pixel values above 50 and below 200). The values that produced the best separation of leaves from background were then applied to all the images in the data set for comparison with data from manually collected leaf areas.

Chronosequence data for leaf and pixel areas were independently fitted to the logistic equation:

$$y = y_0 + \frac{a}{1 + (x/x_0)^b} \quad (1)$$

where x is time, y is the leaf area or pixel area, and the parameters y_0, x_0, a, and b were fitted to data using a least squares method and R, a freely available language and environment for statistical computing and graphics (www.cran.r-project.org).

3. Results

Leaves began to emerge from *R. occidentale* near May 4 in 2004 and two weeks later in 2005 (Fig. 2A and B); leaf expansion in 2005 continued later in the season than for 2004. Mean leaf area per branch increased quickly for the first two weeks and then slowed, reaching a maximum about four weeks after budburst for both years (Fig. 2A). Mean area per leaf increased similarly to that of

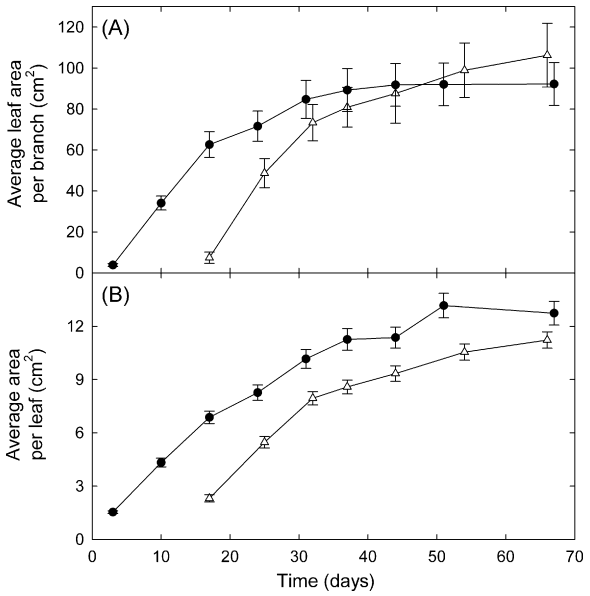

Fig. 2. Mean leaf area per branch (A) and per leaf (B) for manually measured *R. occidentale* branches during the Spring of 2004 (open triangles) and 2005 (closed circles); time is in days relative to the 1st of May. Values are means ± standard errors (n = 36 branches in 2004, each with a mean of 7.6 ± 2.2 [SD] leaves per branch; n = 18 branches in 2005, each with a mean of 10.1 ± 2.5 [SD] leaves per branch).

total leaf area for both years (Fig. 2B). Mean area per leaf was higher in 2004 than in 2005 for specific dates (e.g. June 7; $p < 0.001$, W = 16,511; Wilcoxon rank sum test) but final areas of the largest leaf were not significantly different between years (p = 0.2, W = 393). The mean number of leaves per branch was 7.6 ± 2.2 (mean ± SD, n = 36) for 2004 and 10.2 ± 2.7 (n = 18 branches) for 2005 (p = 0.002; W = 465).

Capturing non-occluded images of target branches were only possible with the horizontal and PTZ mobility of the camera system. Histograms of the frequency of pixels in each color component in both color spaces aided in selecting the upper and lower bounds of color components for image segmentation (Figs. 3 and 4). In the RGB color space, the frequency of pixels that occurred in each color component in images that did not contain leaves (before budburst in May) was maximal near values of 100 (Fig. 3A). The overall color of the images captured before budburst was slightly reddish brown, which is reflected by the peak of the red color component being shifted toward higher values. The color components of images captured at full leaf (in July) have the green component shifted towards higher values (Fig. 3B). Areas in images that were hand-selected to contain only leaves are brighter (all three color components are shifted toward higher values) than are entire images of branches at full leaf (Fig. 3C). Also in these hand-selected areas, the three color components are more separate than occur in entire images. This analysis suggested an initial set of color component values for segmentation. The lower and upper bounds of color component values used for image segmentation were: 89 and 255 for red, 104 and 255 for green, and 77 and 223 for blue, respectively.

In the HSL color space, the frequency of pixels that occurred in the hue color component in images that did not contain leaves (before budburst in May) was approximately evenly distributed among all the hue values (Fig. 4A, solid line); the saturation color component during this time was low and luminance had a low peak at mid-range values (Fig. 4C). The hue of areas within images that were hand-selected to contain only the green buds during this time had a strong peak near a value of 60 (Fig. 4A, dashed line). The hue of entire images captured at full leaf (in July) is similar to those of

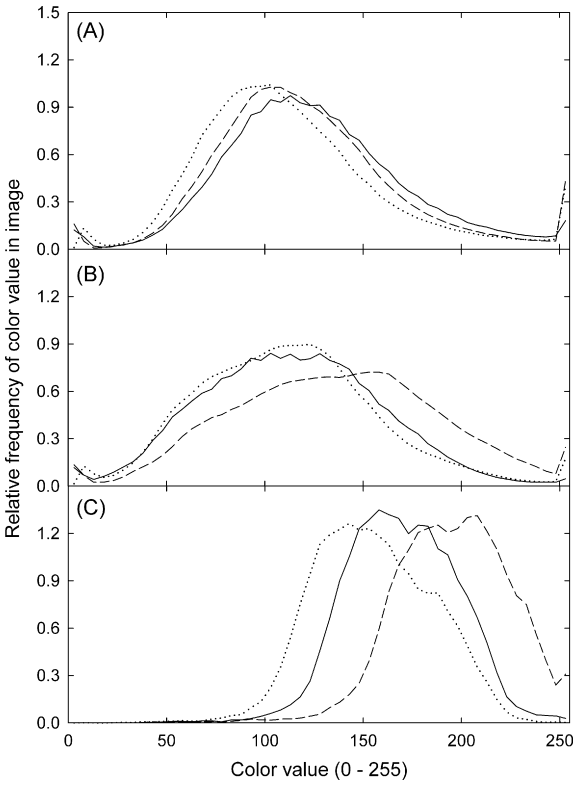

Fig. 3. The mean relative percent frequency of red (solid line), green (dashed line), and blue (dotted line) pixel values in images of *R. occidentale* (A) on 13-May-2005 when no leaves (only green buds) were present and (B) on 6-July-2005 when plants were in full flush ($n = 18$). For comparison, (C) is the relative percent frequency of red, green, and blue pixel values for portions of the 6-July-2005 images that contained leaves only.

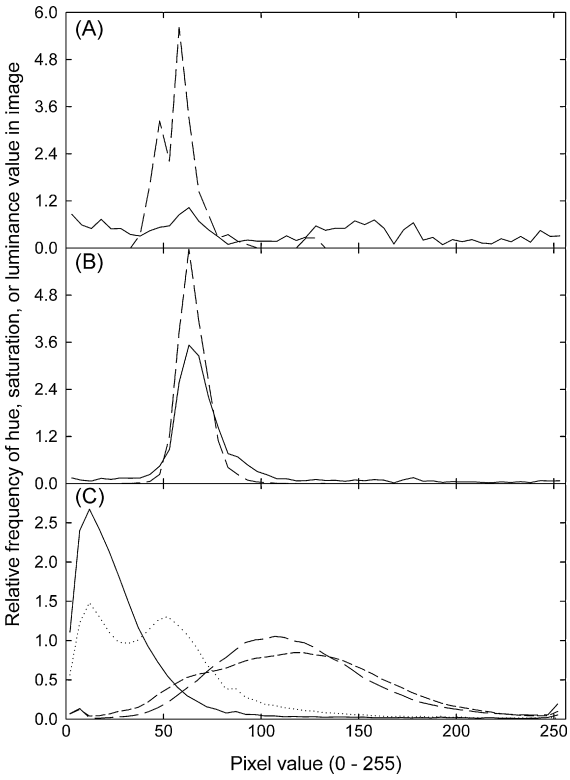

Fig. 4. The mean relative percent frequency of pixel hue values in images of *R. occidentale* (A) on 13-May-2005 when no leaves (only green buds) were present and (B) on 6-July-2005 when plants were in full flush ($n = 18$). For comparison (dashed lines) are the relative percent frequencies for portions of the images that contained the buds or leaves only for those same dates. Values for saturation (solid and dotted lines) and luminance (long dashed and short dashed lines) for entire images captured in May (solid and long dashed lines) and in July (dotted and short dashed lines) are in panel (C).

hand-selected areas that contain only green leaves at that time and similarly has a sharp peak at a value near 60 (Fig. 4B). Mean saturation increased slightly with leaf-out and luminance also shifted to higher values, although not dramatically (Fig. 4C). The lower and upper bounds of color component values used for image segmentation were: 34 and 79 for hue, 12 and 255 for saturation, and 39 and 231 for luminance.

The number of pixels contained in hand-selected areas within images that contained only green leaves corresponded well to the total leaf area measured by hand (Fig. 5A). The mean RMS error was 6.1 cm^2 over the entire time period, calculated by comparing the logistic regressions (Eq. (1)) fitted to each set of data. The two thresholding methods for extracting leaf area information from entire images (RGB-based and HSL-based) were applied to images in the chronosequence with different results (Fig. 5B and C). Hue-based thresholding to isolate leaves from background resulted in a mean RMS error of 21.2 cm^2 with a maximum error of 38.1 cm^2 when comparing the regression to hand-counts of leaf area ($r^2 = 0.837$). RGB-based thresholding to isolate leaves resulted in a mean RMS error of 36.3 cm^2 and a maximum error of 41.4 cm^2 ($r^2 = 0.451$). Parameters fitted to Eq. (1) for each method are indicated in Table 1.

For comparison, using entire images and the algebraic sum of $-R + 2G - B$ as a measure of increasing green in images (Richardson et al., 2007) resulted in a mean RMS error of 99.3 cm^2 with a maximum error of 221.7 cm^2 and an r^2 for a linear best fit regression between leaf area and a green value of 0.579. The optimized algebraic fit to the data was $-3.4R + 2.8G - B$, with a mean RMS error of 97.8 cm^2, a maximum error of 215.5 cm^2, and an r^2 value of 0.591. Using entire images and the color ratio method of mean green:red pixel values to detect the change of green in images (Graham et al., 2006) resulted in a mean RMS error of 122.1 cm^2, a maximum error of 274.6 cm^2, and an r^2 value of 0.364

Exponential regressions for calculating leaf area per branch and total leaf area in entire images from HSL-based pixel counts had r^2 values of 0.817 and 0.802, respectively (Fig. 6A, B). Mean leaf area in the entire image was calculated as the proportion of pixels in hand-selected areas of only green leaves (whose leaf area had been hand-measured in the field) relative to that selected from HSL-based pixel counts in the entire image. Leaf area based on images taken at the end of the growing season of 2004 using the 2005 regression, resulted in a calculated leaf area that was different from hand-measured areas by only -2.12 ± 49.22 cm^2 (SE; $n = 8$ branches).

Sap flow measured in two branches, simultaneous with manually and image-based leaf area measurements, were similar to each other (data shown for one branch only over the course of 70 days; Fig. 7). Estimated leaf area using HSL-based pixel counts very closely matched the hand-measured leaf area for both branches

Table 1
Fitted parameters to the logistic equation (Eq. (1)) for different methods of leaf area estimation based on manual sampling or automated image analysis.

Method	a	b	x_0	y_0
Manually measured leaves	93.68	−5.73	25.13	−1.000
Manually segmented image	94.69	−4.73	22.95	−0.338
Hue-based segmentation	86.96	−6.75	19.03	−0.398
RGB-based segmentation	82.13	−4.58	16.98	−1.000

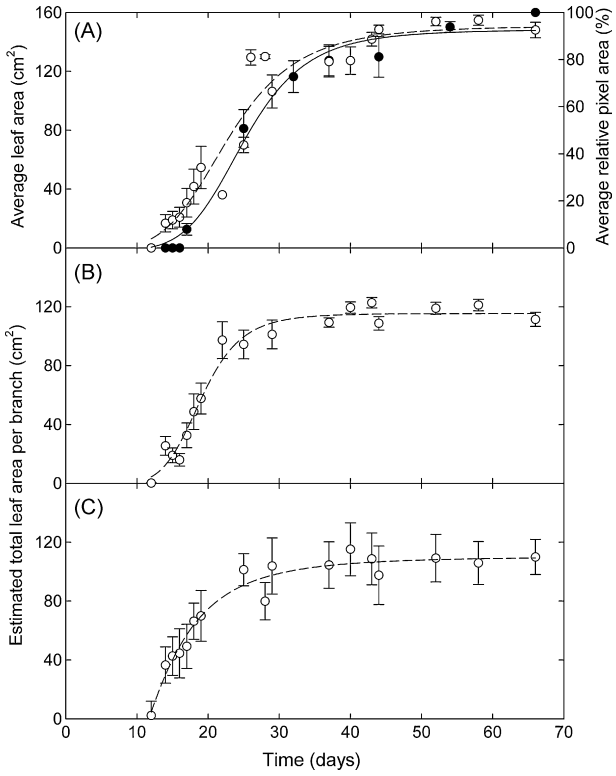

Fig. 5. Time courses for (A) manually collected leaf areas (closed symbols and solid regression line) and pixel counts of areas within images of branches that include only the branch of interest (open symbols and dashed regression line), (B) estimated best-fit leaf areas from images using hue-based masking and (C) RGB-based masking. Time is in days relative to 1-May-2005. Data are means ± standard errors ($n = 18$ branches for manually collected data and $n = 14$ pan-tilt-zoom combinations that capture the 18 manually collected branches).

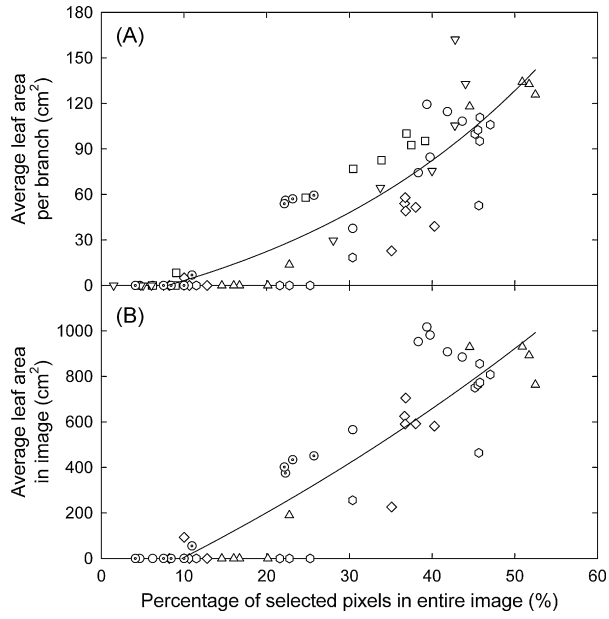

Fig. 6. Regressions for calculating leaf area per branch (A), based on total non-masked area in images and manually collected branch data, and (B) leaf area in the entire image based on the above data transformed by number of pixels contained in the image of only the leaves manually measured as a proportion of the number of pixels in the entire image. Data are for seven unique pan-tilt-zoom combinations (different symbols) during nine image-taking periods during leaf flush.

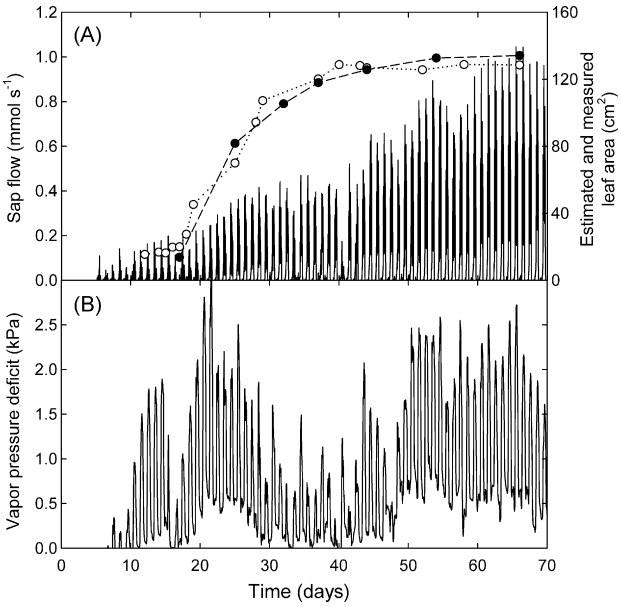

Fig. 7. Time course for (A) sap flow (solid line) in a branch that was also manually measured for leaf area (closed symbols and dashed line) and imaged for leaf area estimations (open symbols and dotted line) and (B) the vapor pressure deficit estimated from hourly mean air temperature (assuming leaf temperature tracks air temperature) and relative humidity measured from a micrometeorological station within 10 m of the site. Time is in days relative to 1-May-2005.

(Fig. 7A). Instantaneous sap flow maxima did not increase in the same manner as leaf area, instead, rising more linearly over this time period. The vapor pressure deficit (the difference in concentration of water vapor in the air, measured as relative humidity, and that inside the leaf, assuming leaf temperature tracked air temperature; VPD) was variable over the 70 d of measurements (Fig. 7B), reflecting diurnal and longer-term changes in air temperature and relative humidity (data not shown). Using the linear relationship between sap flow and the driving force for transpiration (VPD), and setting leaf conductance proportional to leaf area, the calculated maximum water transport more closely matches total leaf area (data not shown).

4. Discussion

Interannual variation in the timing of plant phenological events can be large, with the standard deviation of mean and latest dates of flowering or leafing ranging from days to weeks (Badeck et al., 2004). This is consistent with our observation that *R. occidentale* in the understory of a mixed conifer forest leafed out about 12 days later in 2005 than in 2004. An acceleration of spring phenology has occurred widely in the late 20th century (Walther et al., 2002; Menzel and Fabian, 1999), which has been estimated to be about 5 days per decade (Root et al., 2003). Because other factors such as photoperiod and microenvironment also affect phenology and the response to each abiotic factor can be species-specific (Jame et al., 1998; Schaber and Badeck, 2003), a complex mosaic of phenological responses to anthropogenically induced global climate change can result.

For most deciduous forests in temperate areas, remote sensing data detects the greening of the understory that occurs several weeks before bud burst of the overstory tree leaves (Badeck et al., 2004). Different species within a forest also contribute differently to even the most basic functional aspects of forests, such as water transport (Cienciala et al., 1999). Thus, there is a need to incorporate other, ground-based sensors to relate satellite data to meaning-

ful phenological and physiological phenomena. As an example, sap flow data on *R. occidentale* suggested that the greening of a species as it relates to water transport requires additional meteorological sensor data for interpretation (e.g. the driving force for transpiration is measured as the vapor pressure difference between the leaf and the free air). Thus, multiple sensor modalities must accompany ground-based physiological work on the individual species that comprise a remote sensing pixel. The field of computer vision and robotics clearly offers great opportunities for obtaining such measurements and for the analysis of ecologically important data (Allen et al., 2007; Caron et al., 2008) and comparison to remote sensing data.

Satellite observations can be tied to powerful methods (e.g. normalized difference vegetation index; Reed et al., 1994) for determining spring greening, or "green-up" and for documenting the changes in timing that may be occurring due to global climate change. However, if the causes of changes in surface greenness derived from satellite observations are to be understood, ground-based observations of the phenophase and physiology of individual plants need to be extrapolated to the larger areas that comprise a satellite "pixel" (Badeck et al., 2004). Traditional hand-measurements of phenology are not easily scaleable and thus generally do not provide the spatially integrated response that is easily correlated to the area-averaged information obtained from remote sensing tools.

To better understand the phenological effects in landscapes, methods to identify sources of variation of the area-averaged satellite signals need to be evaluated. One such method, the nesting of finer-resolution images within larger-scale satellite data, has great potential. The inclusion of digital cameras in the design of the newest generation of ecological observatories (e.g. National Ecological Observatory Network, NEON; www.neoninc.org), that feature a diverse set of sensing capabilities and remote observational functions, will enable such a transformation in the scope of environmental research. Observatory networks that utilize a mixture of fixed, wireless, and mobile components will greatly enhance our understanding of global climate shifts and the impacts of local and regional land use changes (Hamilton et al., 2007).

Relatively few plant ecological studies to date have utilized color information from consumer-grade digital cameras as a research tool. Dymond and Trotter (1997) used digital color images of forest and pasture taken from aircraft to determine their reflectance properties, Richardson et al. (2001) examined the spectral reflectance of pine needles along an elevational gradient, and Richardson et al. (2007) tracked spring greenness with a camera, correlated with eddy flux measurements. Analysis of such ecological images has been simple, often to enhance objectivity (Richardson et al., 2007). However, objectivity and inter-comparability between studies can still be maintained while using equally simple but more powerful image processing techniques such as color space transformations and image segmentation.

Image segmentation by color thresholding is a commonly used image processing technique (Cheng et al., 2001; Litwin et al., 2001). The technique demonstrated here, image segmentation by color thresholding in the HSL color space, increased the signal of greening while significantly reducing the error, compared to using algebraic sums, ratios, or the thresholding in the RGB space. Because color transformation is a simple technique, it is recommended that this method be examined in future work with selecting and analyzing areas in images of ecological interest. Even though estimating leaf area based on two-dimensional images can result in errors after the leaf area index has increased to great than one, using non-linear interpretations of image values should partially compensate for this. Additionally, with the use of a mobile camera system, the capacity to capture spatially separated images would allow for stereo analysis. The mobility of the camera in this study allowed for unobstructed imaging of branches along a 30 m transect, a feat that would not have been possible with a fixed camera. The utility of mobility of sensors has been newly recognized by ecologists and has been included in the designs of new classes of environmental observatories (Hamilton et al., 2007).

Acknowledgements

The authors thank Brett L. Jordan and Jason C. Fisher for their assistance with Fig. 1. This research was supported by National Science Foundation award 0120778 to the Center for Embedded Networked Sensing at the University of California, Los Angeles.

References

Allen, M.F., Vargas, R., Graham, E.A., Swenson, W., Hamilton, M., Taggart, M., Harmon, T.C., Rundel, P., Fulkerson, B., Estrin, D., 2007. Soil sensor technology: life within a pixel. BioScience 57, 859–867.

Badeck, F.W., Bondeau, A., Bottcher, K., Doktor, D., Lucht, W., Schaber, J., Sitch, S., 2004. Responses of spring phenology to climate change. New Phytologist 162, 295–309.

Betancourt, J.L., Schwartz, M.D., Breshears, D.D., Brewer, C.A., Frazer, G., Gross, J.E., Mazer, S.J., Reed, B.C., Wilson, B.E., 2007. Evolving plans for the USA National Phenology Network, vol. 88. EOS, Transactions American Geophysical Union, p. 211.

Bruce, J., Balch, T., Veloso, M.M., 2000. Fast and inexpensive color image segmentation for interactive robots. In: Proceedings of the 2000 IEEE/RSJ International Conference on Intelligent Robots and Systems (IROS'00) 3, pp. 2061–2066.

Caron, D.A., Sukhatme, G.S., Kaiser, W.J., Stauffer, B., Oberg, C., Zhang, B., Dhariwal, A., Singh, A., Batalin, M., Moorthi1, S., Pereira, A., Das, J., Graham, E.A., Hansen, M.H., 2008. Macro- to fine-scale spatial and temporal distributions and dynamics of phytoplankton and their environmental driving forces in a small subalpine lake in southern California, USA. Limnology and Oceanography 53, 2333–2349.

Chang, K., Yau, N., Hansen, M.H., Estrin, D., 2006. SensorBase.org—a centralized repository to slog sensor network data. In: Proceedings of the International Conference on Distributed Networks (DCOSS)/EAWMS.

Cheng, H.D., Jiang, X.H., Sun, Y., Wang, J., 2001. Color image segmentation: advances and prospects. Pattern Recognition 34, 2259–2281.

Cienciala, E., Kucera, J., Lindroth, A., 1999. Long-term measurements of stand water uptake in Swedish boreal forest. Agricultural and Forest Meteorology 98–9, 547–554.

Dymond, J.R., Trotter, C.M., 1997. Directional reflectance of vegetation measured by a calibrated digital camera. Applied Optics 36, 4314–4319.

Graham, E.A., Hamilton, M.P., Mishler, B.D., Rundel, P.W., Hansen, M.H., 2006. Use of a networked digital camera to estimate net CO_2 uptake of a desiccation tolerant moss. International Journal of Plant Sciences 167, 751–758.

Hamilton, M.P., Rundel, P.W., Allen, M.F.A., Kaiser, W.J., Hansen, M.H., Estrin, D., 2007. New approaches in embedded networked sensing for terrestrial ecological observatories. Environmental Engineering Science 24, 192–204.

Harmon, T.C., Ambrose, R.F., Gilbert, R.M., Fisher, J.C., Stealey, M., Kaiser, W.J., 2007. High-resolution river hydraulic and water quality characterization using rapidly deployable networked infomechanical systems (NIMS RD). Environmental Engineering Science 24, 151–159.

Hyman, J., Graham, E.A., Hansen, M.H., Estrin, D., 2007. Imagers as sensors: correlating plant CO_2 uptake with digital visual-light imagery. In: 4th International Workshop on Data Management for Sensor Networks, VLDB'07, September 23–28, Vienna, Austria.

ITU, 1992. Information technology – digital compression and coding of continuous-tone still images – requirements and guidelines. In: Recommendation T. 81. International Telecommunication Union, Genève, Switzerland, 186 pp.

Jame, Y.W., Cutforth, H.W., Ritchie, J.T., 1998. Interaction of temperature and daylength on leaf appearance rate in wheat and barley. Agricultural and Forest Meteorology 92, 241–249.

Jolly, W.M., Nemani, R., Running, S.W., 2005. A generalized, bioclimatic index to predict foliar phenology in response to climate. Global Change Biology 11, 619–632.

Jordan, B.L., Batalin, M.A., Kaiser, W.J., 2007. NIMS RD: a rapidly deployable cable based robot. In: IEEE International Conference on Robotics and Automation, Rome, Italy, 10–14 April, 2007, pp. 144–150.

Kansal, A., Yuen, E., Kaiser, W.J., Pottie, G.J., Srivastava, M.B., 2003. Sensing uncertainty reduction using low complexity actuation. In: 2nd International Workshop on Information Processing in Sensor Networks (IPSN'03), Palo Alto, CA, April 2003.

Litwin, D., Tjahjadi, T., Yang, Y.-H., 2001. Colour image segmentation using optical models. In: Pluta, M. (Ed.), Proceedings of SPIE in Optical Sensing for Public Safety, Health, and Security, vol. 4535, pp. 137–144.

Liu, J.G., Moore, J.McM., 1990. Hue image RGB colour composition. a simple technique to suppress shadow and enhance spectral signature. International Journal of Remote Sensing 11, 1521–1530.
Menzel, A., Fabian, P., 1999. Growing season extended in Europe. Nature 397, 659.
Menzel, A., 2002. Phenology: its importance to the global change community. Climatic Change 54, 379–385.
Pon, R., Batalin, M., Gordon, J., Kansal, A., Liu, D., Rahimi, M., Shirachi, L., Yu, Y., Hansan, M.H., Kaiser, W.J., Srivastava, M., Sukhatme, G., Estrin, D., 2005. Networked infomechanical systems: a mobile embedded networked sensor platform. In: IEEE/ACM Fourth International Conference on Information Processing in Sensor Networks, pp. 376–381.
Pratt, W.K., 2001. Digital Image Processing, 3rd ed. John Wiley & Sons, Inc., New York, p. 84.
Rahimi, M.S., Ahmadian, S., Zats, D., Laufer, R., Estrin, D., 2006. Magic of numbers in networks of wireless image sensors. In: Workshop on Distributed Smart Cameras (DSC), 2006.
Rahimi, M., Hansen, M.H., Kaiser, W.J., Sukhatme, G.S., Estrin, D., 2005. Adaptive sampling for environmental field estimation using robotic sensors. In: Proceedings IEEE/RSJ International Conference on Intelligent Robots and Systems (IROS), 2–6 August 2005, pp. 3692–3698.
Reed, B.C., Brown, J.F., Vanderzee, D., Loveland, T.R., Merchant, J.W., Ohlen, D.O., 1994. Measuring phenological variability from satellite imagery. Journal of Vegetation Science 5, 703–714.
Richardson, A.D., Berlyn, G.P., Gregoire, T.G., 2001. Spectral reflectance of Picea rubens (Pinaceae) and Abies balsamea (Pinaceae) needles along an elevational gradient, Mt. Moosilauke, New Hampshire, USA. American Journal of Botany 88, 667–676.
Richardson, A.D., Jenkins, J.P., Braswell, B.H., Hollinger, D.Y., Ollinger, S.V., Smith, M.-L., 2007. Use of digital webcam images to track spring green-up in a deciduous broadleaf forest. Oecologia 152, 323–334.
Root, T.L., Price, J.T., Hall, K.R., Schneider, S.H., Rosenzweig, C., Pounds, J.A., 2003. Fingerprints of global warming on wild animals and plants. Nature 421, 57–60.
Schaber, J., Badeck, F.W., 2003. Physiology-based phenology models for forest tree species in Germany. International Journal of Biometeorology 47, 193–201.
Slayback, D.A., Pinzon, J.E., Los, S.O., Tucker, C.J., 2003. Northern hemisphere photosynthetic trends 1982–99. Global Change Biology 9, 1–15.
Stöckli, R., Vidale, P.L., 2004. European plant phenology, climate as seen in a 20 year AVHRR land-surface parameter dataset. International Journal of Remote Sensing 25, 3303–3330.
Walther, G.R., Post, E., Convey, P., Menzel, A., Parmesan, C., Beebee, T.J.C., Fromentin, J.M., Hoegh-Guldberg, O., Bairlein, F., 2002. Ecological responses to recent climate change. Nature 416, 389–395.
Wright, S.J., Carrasco, C., Calderón, C., Paton, S., 1999. The El Niño southern oscillation, variable fruit production, and famine in a tropical forest. Ecology 80, 1632–1647.
Zhang, B., Sukhatme, G.S., 2007. Adaptive sampling for estimating a scalar field using a robotic boat and a sensor network. In: Robotics and Automation, 2007 IEEE International Conference, 10–14 April 2007, pp. 3673–3680.